

# Nanoscale

Accepted Manuscript



This is an *Accepted Manuscript*, which has been through the Royal Society of Chemistry peer review process and has been accepted for publication.

*Accepted Manuscripts* are published online shortly after acceptance, before technical editing, formatting and proof reading. Using this free service, authors can make their results available to the community, in citable form, before we publish the edited article. We will replace this *Accepted Manuscript* with the edited and formatted *Advance Article* as soon as it is available.

You can find more information about *Accepted Manuscripts* in the [Information for Authors](#).

Please note that technical editing may introduce minor changes to the text and/or graphics, which may alter content. The journal's standard [Terms & Conditions](#) and the [Ethical guidelines](#) still apply. In no event shall the Royal Society of Chemistry be held responsible for any errors or omissions in this *Accepted Manuscript* or any consequences arising from the use of any information it contains.



## Nanoscale

## ARTICLE

## Effect of Magnetic Field Strength on the Alignment of $\alpha''$ -Fe<sub>16</sub>N<sub>2</sub> Nanoparticle Films

Christina W. Kartikowati,<sup>a</sup> Asep Suhendi,<sup>a,b</sup> Rizka Zulhijah,<sup>a</sup> Takashi Ogi,<sup>a</sup> Toru Iwaki,<sup>a</sup> and Kikuo Okuyama<sup>a</sup>

Received 00th January 20xx,  
Accepted 00th January 20xx

DOI: 10.1039/x0xx00000x

www.rsc.org/

Aligning the magnetic orientation is one strategy to improve the magnetic performance of magnetic materials. In this study, well-dispersed single-domain core-shell  $\alpha''$ -Fe<sub>16</sub>N<sub>2</sub>/Al<sub>2</sub>O<sub>3</sub> nanoparticles (NPs) were aligned by vertically applying magnetic fields with various strengths to a Si wafer substrate followed by fixation with resin. X-ray diffraction indicated that the alignment of the easy *c*-axis of the  $\alpha''$ -Fe<sub>16</sub>N<sub>2</sub> crystal and the magnetic orientation of the NPs depended upon the applied magnetic field. Magnetic analysis demonstrated that increasing the magnetic field strength resulted in hysteresis loops approaching a rectangular form, implying a higher magnetic coercivity, remanence, and maximum energy product. The same tendency was also observed when a horizontal magnetic field was applied. The fixation of the easy *c*-axis alignment of each nanoparticle caused by Brownian rotation under the magnetic field, instead of Néel rotation, was the reason for the enhancement in the magnetic performance. These results on the alignment of the magnetic orientation of  $\alpha''$ -Fe<sub>16</sub>N<sub>2</sub> nanoparticles suggest the practical application of high-performance permanent bulk magnets from well-dispersed single-domain  $\alpha''$ -Fe<sub>16</sub>N<sub>2</sub>/Al<sub>2</sub>O<sub>3</sub> NPs.

### Introduction

Ferromagnetic FePt nanoparticles (NPs) ranging in size from single to several tens of nanometers and SmCo, NdFeB, and Fe<sub>16</sub>N<sub>2</sub> NPs have been widely studied, and much research has focused on the functionalization of NP assemblies.<sup>1–4</sup> Such magnetic NP assemblies are expected to provide high-performance magnetic materials for practical applications in new nanotechnologies such as ultrahigh-density recording media, high-performance nanocomposite bulk magnets, biomedical materials, spintronic devices, and environmentally friendly technologies.<sup>5–12</sup> Different applications require NP assemblies with different magnetic properties. Precise control of the magnetic properties of NP assemblies is therefore highly necessary.<sup>13</sup> Control of their magnetic properties enables NP assemblies to be used in a wider range of advanced applications.

Recently, rare-earth-free high-magnetic-moment NPs, namely single-domain ferromagnetic spherical  $\alpha''$ -Fe<sub>16</sub>N<sub>2</sub> NPs have been successfully synthesized.<sup>2, 14–16</sup> As rare-earth-free magnetic material,  $\alpha''$ -Fe<sub>16</sub>N<sub>2</sub> NPs have a theoretical BM product of 130 MGOe. This implies that this NPs are a prospective magnetic material, although the present *H<sub>c</sub>* value

is not as high as those of the rare-earth materials. The  $\alpha''$ -Fe<sub>16</sub>N<sub>2</sub> phase was formed by nitriding core-shell  $\alpha$ -Fe NPs that were prepared directly using a plasma method. It was expected that assembled magnetic films or bulk materials with higher magnetizations and coercivities, in which  $\alpha''$ -Fe<sub>16</sub>N<sub>2</sub> NPs are isolated as single-domain particles covered with non-magnetic materials such as Al<sub>2</sub>O<sub>3</sub> or SiO<sub>2</sub>, could be obtained.

Several methods have been widely used for the preparation of  $\alpha''$ -Fe<sub>16</sub>N<sub>2</sub> films, including sputtering, ion beam deposition, nitrogen-ion implantation, tempering nitride-based bulk martensite, and dip coating.<sup>17, 18</sup> However it is difficult to form a pure  $\alpha''$ -Fe<sub>16</sub>N<sub>2</sub> phase (other Fe–N phases are present, affecting the magnetic properties) and to control the magnetic moment orientation of the film to improve the magnetic performance. Control of the magnetic moment orientation, simply called the magnetic orientation, of magnetic NP assemblies is therefore still a challenge and crucial for the development of new nanostructured magnets.

Our group successfully prepared a ferrofluid of well-dispersed core-shell  $\alpha''$ -Fe<sub>16</sub>N<sub>2</sub>/Al<sub>2</sub>O<sub>3</sub> NPs by a low-energy bead-mill dispersion method.<sup>19</sup> A new route to form a ferromagnetic film from rare-earth-free well-dispersed  $\alpha''$ -Fe<sub>16</sub>N<sub>2</sub> NPs with the presence and absence of an applied magnetic field was established.<sup>20</sup> The applied magnetic field aligned the easy *c*-axis and magnetic orientation of the NPs, resulting in the enhancement of the magnetic performance of the film. The magnetic remanence ratio (*M<sub>r</sub>*/*M<sub>s</sub>*) and coercivity (*H<sub>c</sub>*) increased by 55.2% and 24%, respectively upon the application of a 1.2 T magnetic field. However, the effects of

<sup>a</sup> Department of Chemical Engineering, Graduate School of Engineering, Hiroshima University, 1-4-1 Kagamiyama, Higashi Hiroshima 739-8527, Japan. E-mail: ogit@hiroshima-u.ac.jp; Tel: +81-82-424-7850; Fax: +81-82-424-5494

<sup>b</sup> Program Studi Teknik Fisika, Fakultas Teknik Elektro, Telkom University, Jl. Telekomunikasi Terusan Buah Batu, Bandung 40257, Indonesia.

the magnetic field on the magnetic orientation of the NP films and their magnetic properties were not examined. As a continuation of our previous studies,<sup>20</sup> we have focused on the control of the magnetic orientation during the synthesis of  $\alpha''$ -Fe<sub>16</sub>N<sub>2</sub> films using well-dispersed  $\alpha''$ -Fe<sub>16</sub>N<sub>2</sub> NPs and analyzed the relationship between the aligned magnetic orientation of the NPs and their magnetic properties, using newly prepared  $\alpha''$ -Fe<sub>16</sub>N<sub>2</sub> NPs.

In this study,  $\alpha''$ -Fe<sub>16</sub>N<sub>2</sub> NP films were prepared by spin-coating, using the same method as in our previous study.<sup>20</sup> Magnets with various magnetic field strengths up to 1.2 T were applied during the film formation to align the magnetic orientation of the assembled NPs in the same direction before fixing the NPs in the film with epoxy resin binder. The magnetic properties such as the magnetic coercivity ( $H_c$ ), magnetic remanence ( $M_r$ ), maximum energy product  $[(BH)_{max}]$ , and anisotropic magnetic field ( $H_k$ ) of the prepared  $\alpha''$ -Fe<sub>16</sub>N<sub>2</sub> NP films show that the control of the magnetic orientation improves the performance of the resulting magnetic materials. The magnetic properties of the  $\alpha''$ -Fe<sub>16</sub>N<sub>2</sub> NP films show the potential for the nanostructuring of bulk magnetic materials with controllable magnetic properties.

## Experimental

### Preparation of magnetically aligned films

The synthesis of ferromagnetic core-shell  $\alpha''$ -Fe<sub>16</sub>N<sub>2</sub>/Al<sub>2</sub>O<sub>3</sub> NPs by the nitridation of core-shell  $\alpha$ -Fe/Al<sub>2</sub>O<sub>3</sub> using a plasma method was described in our previous report.<sup>2, 14, 16</sup> A concentrated ferrofluid containing  $\alpha''$ -Fe<sub>16</sub>N<sub>2</sub>/Al<sub>2</sub>O<sub>3</sub> NPs dispersed in toluene (59 wt%), prepared by low-energy bead-mill dispersion,<sup>19</sup> was mixed with epoxy resin (3,4-epoxycyclohexylmethyl 3,4-epoxycyclohexanecarboxylate) as an NP binder, in a mass ratio of 1:1. The mixed solution was dropped onto a silica (Si) wafer and coated using a spin-coater (Mikasa 1H-D7, Japan) at 300 and 1000 rpm for 30 and 10 s, respectively, as previously described.<sup>20</sup> After the formation of the thin film on the Si wafer, magnetic fields of strength 0, 0.6, 0.9, and 1.2 T were applied before removing the toluene from the coated film. The magnetically aligned NP film was dried and completely fixed with the resin, and then the magnetic field was removed. Details of the preparation of the magnetically aligned core-shell  $\alpha''$ -Fe<sub>16</sub>N<sub>2</sub>/Al<sub>2</sub>O<sub>3</sub> NP film are shown in Fig. 1, and details of the applied magnetic fields used in preparing the various samples are listed in Table 1. The raw materials such as epoxy resin were purchased from Sigma Aldrich (China) and toluene (99.95%) was purchased from Kanto Chemicals (Japan). These raw materials were used without further treatment or purification.

### Characterization

The morphologies of the prepared  $\alpha''$ -Fe<sub>16</sub>N<sub>2</sub>/Al<sub>2</sub>O<sub>3</sub> NP films were observed using field-emission scanning electron microscopy (FE SEM; Hitachi S-5000, Japan) and transmission electron microscopy (TEM; JEM-300F, JEOL Co., Ltd., Japan). The crystalline structures of the films were examined using X-

ray diffraction (XRD; D2 Phaser, Bruker, Germany). The magnetic properties were evaluated using a superconducting quantum interference device (SQUID; Quantum Design, USA). Magnetization was measured as a function of the applied field from 1 to 50 kOe at 300 K.

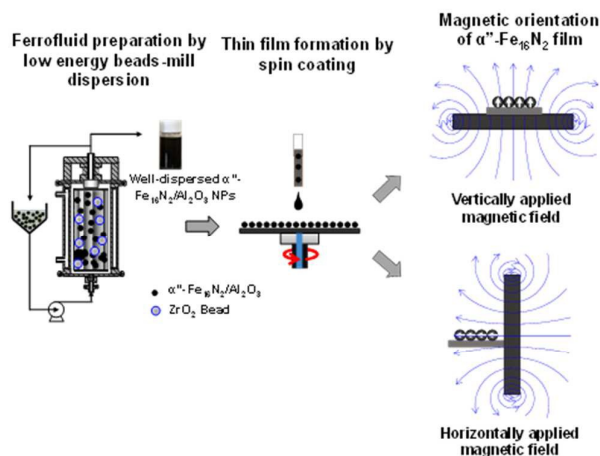


**Fig. 1** Schematic diagram of preparation of magnetically aligned  $\alpha''$ -Fe<sub>16</sub>N<sub>2</sub>/Al<sub>2</sub>O<sub>3</sub> NPs film.

**Table 1.** Applied Magnetic Fields Used in Preparing Various Samples

Sample	Applied magnetic field	
	Magnetic field, H (T)	Direction
V0	0	-
V1	0.6	vertical
V2	0.9	vertical
V3	1.2	vertical
H	0.6	horizontal
R	0 (powder)	-

## Results and Discussion

Fig. 2 shows SEM (a) and TEM (b) images of core-shell  $\alpha''$ -Fe<sub>16</sub>N<sub>2</sub>/Al<sub>2</sub>O<sub>3</sub> NPs. The SEM image shows the as-prepared NPs, and the TEM image shows the NPs after bead-mill dispersion. The inset figure shows the cross-sectional TEM image after bead-mill dispersion. The particles are single-domain NPs of an average size of approximately 50 nm, with a shell thickness of 4 nm. Because the  $\alpha''$ -Fe<sub>16</sub>N<sub>2</sub>/Al<sub>2</sub>O<sub>3</sub> NPs were prepared by the gas phase method at high temperature, it is very difficult to obtain monodisperse NPs. The NP samples were similar to those described in our recent study.<sup>20</sup>

Fig. 3a shows a SEM image of the surface of the spin-coated core-shell  $\alpha''$ -Fe<sub>16</sub>N<sub>2</sub>/Al<sub>2</sub>O<sub>3</sub> NP film under a vertically applied magnetic field, viewed at a tilt angle of 40°. The film surface is wavy because of the thickness of the resin. The film surface was covered with resin to maintain the NP arrangement in the film, as shown in Fig. 3b, which shows a cross-section of a densely packed core-shell  $\alpha''$ -Fe<sub>16</sub>N<sub>2</sub>/Al<sub>2</sub>O<sub>3</sub>

NP film of thickness  $\sim 1 \mu\text{m}$ . The dense packing of the  $\alpha''\text{-Fe}_{16}\text{N}_2/\text{Al}_2\text{O}_3$  NPs in the film is clearly observed. This packing results from the well-dispersed state of the spherical NPs.

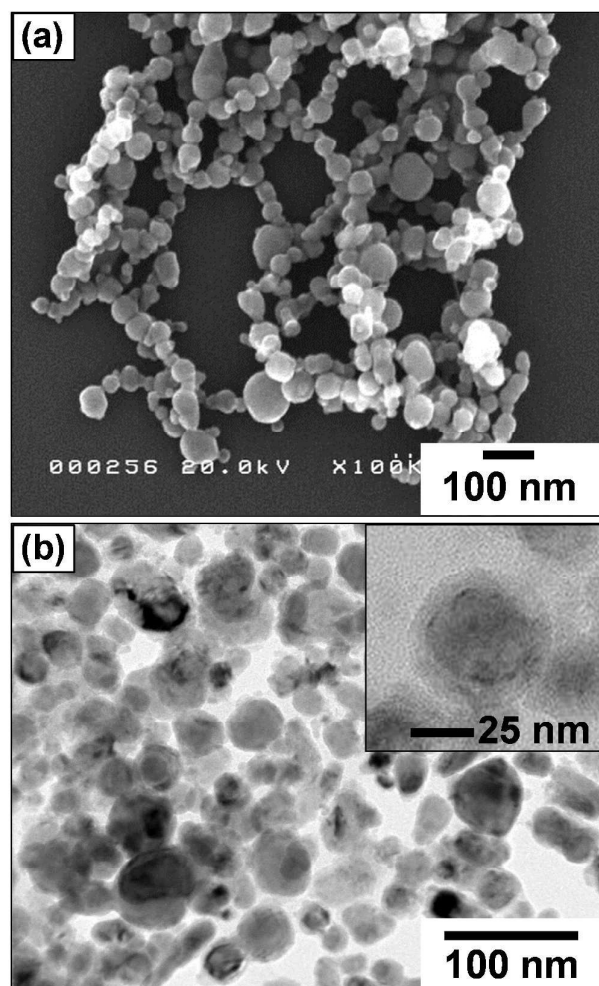


**Fig. 2** SEM and TEM images of  $\alpha''\text{-Fe}_{16}\text{N}_2/\text{Al}_2\text{O}_3$  NPs; inset shows cross-sectional TEM image.

The alignment of the magnetic orientation of  $\alpha''\text{-Fe}_{16}\text{N}_2$  NPs can be carried out using two strategies, i.e., aligning the magnetic orientation and aligning the easy  $c$ -axis of the particle. Aligning the easy  $c$ -axis, simply called the  $c$ -axis, of the particle is preferable due to the lower energy required. However, this strategy is applicable for only well-dispersed particles, where each of the particles can move freely. In the case of agglomerated particles, the alignment of the magnetic orientation can be performed only by the first strategy. Consequently, alignment of the magnetic orientation in agglomerated particles requires high energy.

XRD was used to determine the alignment of the easy  $c$ -axis of the  $\alpha''\text{-Fe}_{16}\text{N}_2$  NP crystal inside the film. Due to the rotation of the particle (Brownian rotation) during the alignment process, the  $c$ -axis and the magnetic orientation of

the particles were aligned in the same direction along the magnetic field. In other words, the alignment of the  $c$ -axis represents the alignment of the magnetic orientation. Fig. 4 shows typical XRD patterns of core-shell  $\alpha''\text{-Fe}_{16}\text{N}_2/\text{Al}_2\text{O}_3$  NP powder and films; the vertical magnetic fields applied to the films varied from 0 to 1.2 T. A comparison of the XRD pattern of the  $\alpha''\text{-Fe}_{16}\text{N}_2/\text{Al}_2\text{O}_3$  NP film without an applied magnetic field (sample V0) with that of the powder (R) shows that the (103), (213), (004), and (224) diffraction peaks of  $\alpha''\text{-Fe}_{16}\text{N}_2$  disappeared in the film. For the films with higher vertically applied magnetic fields (samples V1, V2, and V3), (004) and (224) diffraction peaks of  $\alpha''\text{-Fe}_{16}\text{N}_2$  appeared, and their intensities increased with the increasing magnetic field strength, whereas the (220) intensity decreased significantly, as shown in Fig. 4.

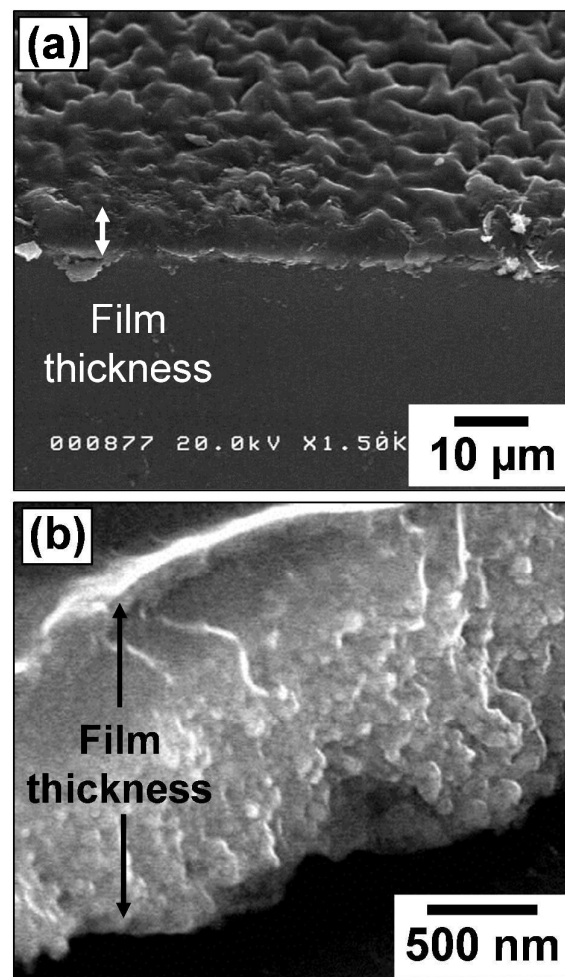


**Fig. 3** SEM images of surface and cross-section of spin-coated  $\alpha''\text{-Fe}_{16}\text{N}_2/\text{Al}_2\text{O}_3$  NP film under vertical magnetic field, viewed at a tilt angle of  $40^\circ$ : low (a) and high (b) magnification.

The (004) peak has a vertical direction along the  $c$ -axis direction. If the (004) peak increased, it means that more of

the *c*-axes of the particles are aligned in the vertical direction. From Fig. 4, the intensity of the (004) diffraction peak of samples V1, V2, and V3 increased, which shows the vertical alignment of the NPs. However, the horizontal direction was shown by the (220) peak. This explains why the (220) peak decreased upon increasing the applied magnetic field strength, which means that the vertically aligned *c*-axis increased. However, the presence of (103) and (224) peaks shows that not all the *c*-axes are aligned perfectly in the vertical direction. The disappearance of the (400) peak in the pattern of the vertically aligned film suggests that no *c*-axes are aligned in the horizontal direction.

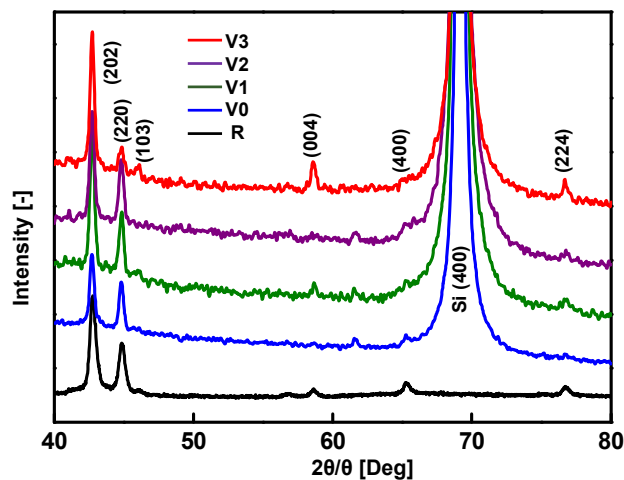


**Fig. 4** XRD patterns of  $\alpha''$ -Fe<sub>16</sub>N<sub>2</sub>/Al<sub>2</sub>O<sub>3</sub> NPs and films under various applied magnetic fields.

The degree of alignment of the magnetic orientation or *c*-axis, which is generally represented by the Lotgering factor (LF), can be calculated from the intensities of the XRD peaks, obtained in the conventional  $2\theta/\theta$  scanning mode, using the following equation:<sup>21</sup>

$$LF = \frac{p - p_0}{1 - p_0} \quad (1)$$

where *p* is the ratio of the summation of the peak intensities corresponding to the preferred orientation axis to the summation of all the diffraction peaks in particle-oriented materials; *p*<sub>0</sub> is the *p* of a material with a random particle distribution.

The LF values were calculated using the above equation from the intensities of the (004) and (224) peaks because those peaks have a vertical direction. Therefore, the degree of *c*-axis alignment can be evaluated from the enhancement of their intensity upon increasing the vertical magnetic field strength.

The LF values of the vertically aligned *c*-axis increased to 35% when the magnetic field was increased to 1.2 T (V3), as shown in Table 2. These results show that 35% of the  $\alpha''$ -Fe<sub>16</sub>N<sub>2</sub> NPs in the film were vertically aligned; therefore, a stronger magnetic field is necessary to increase the alignment of the *c*-axis of the NPs in the film. It was estimated that an 11 T

magnetic field would be needed to perfectly align the *c*-axis in the vertical direction. Contrary to the case where a magnetic field was applied during the synthesis of NPs, the application of a magnetic field during film preparation did not affect the morphology, crystal structure, or magnetic domain structure of the  $\alpha''$ -Fe<sub>16</sub>N<sub>2</sub>/Al<sub>2</sub>O<sub>3</sub> NPs.<sup>22–26</sup> Instead, it only aligned the magnetic orientation and *c*-axis of the NPs along the magnetic field direction.

An LF value of 28% was obtained for the film prepared without a magnetic field (sample V0), showing that the alignment of the magnetic orientation of the NPs occurred even when no magnetic field was applied. This alignment may arise from magnetic interactions between NPs, forming a chain with a head-to-tail arrangement of magnetic dipole moments.<sup>12, 27</sup> This alignment was parallel to the Si wafer due to surface interactions between the NPs and the Si wafer. The SEM image in Fig. 2 confirms that the  $\alpha''$ -Fe<sub>16</sub>N<sub>2</sub> NPs form a chain as a result of the magnetic interactions between particles. The LF values of all the samples and their directions are summarized in Table 2.

**Table 2.** Orientations of Vertically Aligned  $\alpha''$ -Fe<sub>16</sub>N<sub>2</sub> NP Films

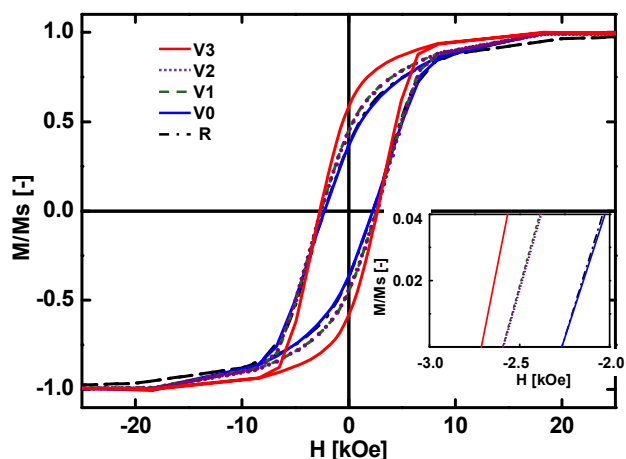
Sample	Alignment [LF (%)]
R	0
V0	28
V1	33
V2	33
V3	35

Fig. 5 shows the magnetic hysteresis loops of the randomly and vertically aligned films obtained by SQUID measurements at 300 K; these have been corrected by the effect of demagnetization. For each *M*–*H* loop, the magnetization is normalized by the saturation magnetization (*M*<sub>s</sub>) of the film. The shape of the hysteresis loops approaches rectangular with the increase in the applied magnetic field, as clearly shown in the figure. A complete alignment of the *c*-axis of the NPs should ideally result in a rectangular hysteresis loop with a magnetic remanence ratio (*M*<sub>r</sub>/*M*<sub>s</sub>) = 1. The saturation magnetization values of the films were ~409 emu/cc or 124.54 emu/gr film, and the magnetic coercivity (*H*<sub>c</sub>) and remanence (*M*<sub>r</sub>) values of the vertically aligned film increased by 24% and 66%, respectively, upon increasing the applied magnetic field to 1.2 T. This increase in *H*<sub>c</sub> and *M*<sub>r</sub> is strongly related to the *c*-axis rotation phenomenon.

The *c*-axis rotation phenomenon was different for well-dispersed and aggregated NPs. The differences in the alignment phenomena of the magnetic orientation upon applying a magnetic field between well-dispersed and agglomerated NPs are illustrated in Table 3.

In the case of well-dispersed NPs, the particles are able to move freely, forming magnetic dipole coupling among NPs. By applying a magnetic field, the *c*-axis of the particle will be easily aligned, where in the case of single domain  $\alpha''$ -Fe<sub>16</sub>N<sub>2</sub>

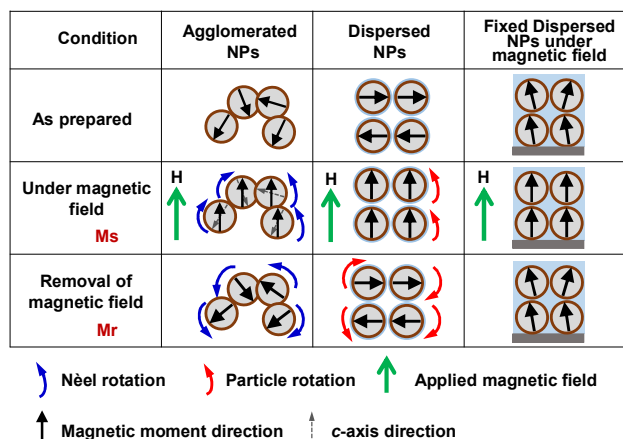
NPs, the alignment of the  $c$ -axis means the alignment of its magnetic orientation. This means that the magnetic orientation and  $c$ -axis have the same direction. However, if the NPs were agglomerated, a higher energy is required to align the magnetic orientation of the NPs because the particle cannot move freely. In other words, only Néel rotation will occur instead of particle rotation. This means that the magnetic orientation and the  $c$ -axis have different directions.



**Fig. 5** Hysteresis loops of  $\alpha''$ - $\text{Fe}_{16}\text{N}_2/\text{Al}_2\text{O}_3$  NPs and films under various applied magnetic fields; inset shows changes in coercivity ( $H_c$ ).

By aligning the magnetic orientation of the well-dispersed  $\alpha''$ - $\text{Fe}_{16}\text{N}_2$  NPs under a magnetic field and then fixing it using resin, the magnetic orientation and the  $c$ -axis will be aligned in the same direction, along the magnetic field. This alignment of the magnetic orientation results in an increase in the magnetic remanence of the film, as shown in the illustration in Table 3. The alignment of the magnetic orientation of the particles influences the rotation of the magnetic moment during SQUID measurement, resulting in a different hysteresis curve. Applying a magnetic field results in an improvement of the magnetic performance of the film, i.e., magnetic remanence ( $M_r$ ) and coercivity ( $H_c$ ).

**Table 3.** Illustration of alignment phenomena of magnetic orientation in the agglomerated and well-dispersed magnetic NPs



The increase in both the  $H_c$  and  $M_r/M_s$  values with the  $c$ -axis alignment was also observed on  $\text{SmCO}_5$  NPs, where a strong magnetic interaction occurred among isolated nanoparticles.<sup>10</sup> The magnetic properties of the agglomerated  $\alpha''$ - $\text{Fe}_{16}\text{N}_2$  films were higher than those of the well-dispersed film, likely due to the effects of the resin present in the film, which is a nonmagnetic material.<sup>28-30</sup>

Significantly higher energy products  $[(BH)_{\text{max}}]$  were also obtained for the  $\alpha''$ - $\text{Fe}_{16}\text{N}_2$  films under a magnetic field than for that without a magnetic field; for example,  $(BH)_{\text{max}}$  values up to 1.211 MGOe were obtained for the film prepared using a magnetic field of 1.2 T, compared with a  $(BH)_{\text{max}}$  value of 0.465 MGOe for the film prepared without a magnetic field. These  $(BH)_{\text{max}}$  values are considerably lower than that of the  $\alpha''$ - $\text{Fe}_{16}\text{N}_2$  NPs, which is 2.029 MGOe. This increase in the maximum energy product occurs because the film consists of well-dispersed NPs; as we previously reported,<sup>19</sup> the  $H_c$  value of well-dispersed  $\alpha''$ - $\text{Fe}_{16}\text{N}_2$  NPs is smaller than that of agglomerated particles because of the strong exchange interactions among the particles.<sup>31</sup> The  $(BH)_{\text{max}}$  for an applied magnetic field of 0.9 T was slightly lower, possibly because of the deviation in the estimation of the film volume. Because  $(BH)_{\text{max}}$  strongly depends on the magnetic coercivity, the application of a stronger magnetic field, which increases the coercivity, also increases  $(BH)_{\text{max}}$ .

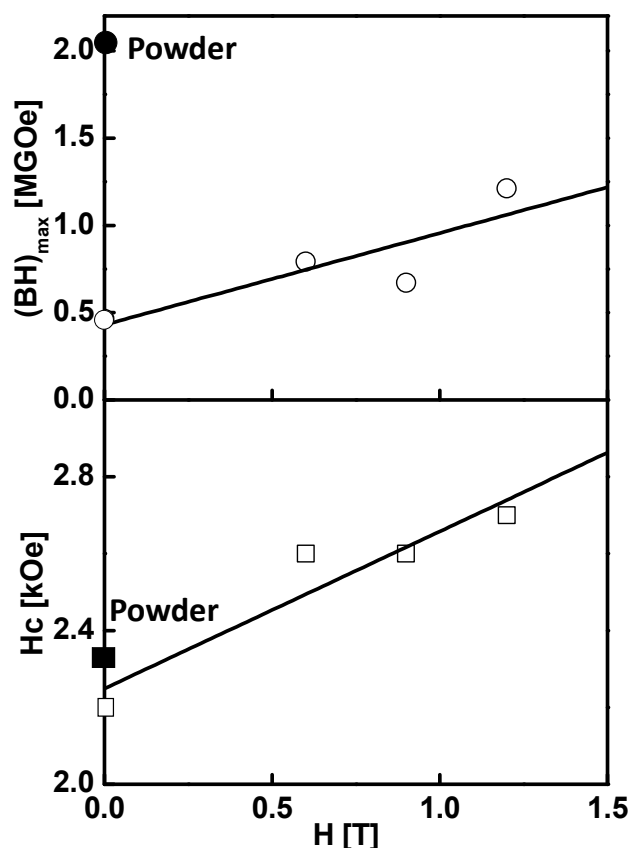


**Fig. 6** Maximum energy product and magnetic coercivity of the  $\alpha''\text{-Fe}_{16}\text{N}_2/\text{Al}_2\text{O}_3$  NP film as a function of the applied magnetic field.

The application of a 1.2 T magnetic field decreased the magnetic anisotropy field ( $H_k$ ) of the  $\alpha''\text{-Fe}_{16}\text{N}_2$  oriented film by 2.7% to  $4.3 \times 10^5$  A/m. This decrease in  $H_k$  corresponds to a magnetocrystalline anisotropy constant ( $K_u$ ) of  $1.11 \times 10^6$  erg/cm<sup>3</sup>. This value was slightly lower than that of the  $\alpha''\text{-Fe}_{16}\text{N}_2$  NP powder, which is  $1.14 \times 10^6$  erg/cm<sup>3</sup>. The magnetic anisotropy is intimately linked to the crystal structure.<sup>32</sup> The alignment of the easy  $c$ -axis of the NP crystal causes a decrease in the magnetic anisotropy. The decrease in the anisotropy constant upon the application of a magnetic field up to 1.2 T confirms that the NP alignment was along the easy  $c$ -axis. The effect of the magnetic field strength on these magnetic properties of  $\alpha''\text{-Fe}_{16}\text{N}_2$  films are shown in Fig. 6. These results confirm that the alignment of the magnetic moment of the particles in the film significantly enhances its magnetic performance. Application of a magnetic field during the synthesis of the magnetic NPs also enhanced the magnetic properties of the prepared NPs.<sup>33</sup>

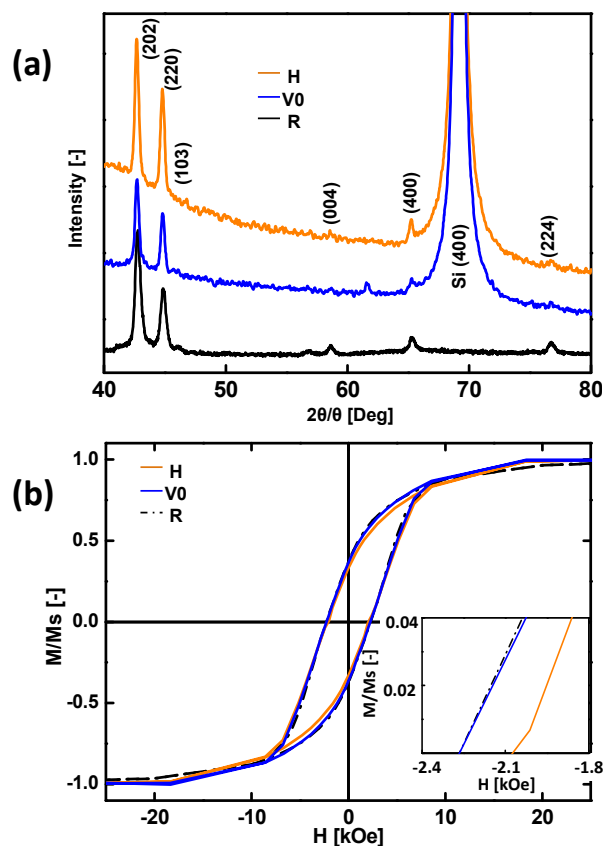


**Fig. 7** XRD pattern (a) and magnetic hysteresis loop (b) of  $\alpha''\text{-Fe}_{16}\text{N}_2/\text{Al}_2\text{O}_3$  NP film under a horizontally applied magnetic field.

For comparison, we synthesized an  $\alpha''\text{-Fe}_{16}\text{N}_2/\text{Al}_2\text{O}_3$  magnetic film under a horizontal magnetic field of 0.6 T. Fig. 7a and b show the XRD patterns and hysteresis loops, respectively, of the horizontally aligned (sample H)  $\alpha''\text{-Fe}_{16}\text{N}_2/\text{Al}_2\text{O}_3$  film and the film prepared without a magnetic field (sample V0). For the horizontally aligned film, (224) and (400)  $\alpha''\text{-Fe}_{16}\text{N}_2$  diffraction peaks were observed, and the intensity of the (220) peak was higher than that for randomly aligned and vertically aligned films, which are shown in Fig. 4. The appearance of a (400) peak for the horizontally aligned film suggests that there are  $c$ -axes of the particles aligned in the horizontal direction. The horizontally aligned film shows a higher-intensity (220) peak, indicating that many  $c$ -axes are aligned in the horizontal direction.

For comparison with the vertically aligned film, the degree of alignment of the magnetic orientation, LF, of the horizontally aligned film was evaluated from the intensities of the (004) and (224) diffraction peaks. The LF value was 27%. The smaller LF value than those for the randomly and vertically aligned films confirms that the  $c$ -axis of the particles was aligned in the horizontal direction. This value of LF is in the vertical direction, meaning that the NPs were 73% horizontally aligned. The XRD pattern of sample H shows that the intensity ratio of the (202) and (220)  $\alpha''\text{-Fe}_{16}\text{N}_2$  NPs diffraction peaks was similar to that of sample V0 (without a magnetic field), which is shown in Fig. 4. This indicates that the  $c$ -axes of the

NPs in the film prepared without a magnetic field were aligned in the horizontal direction.

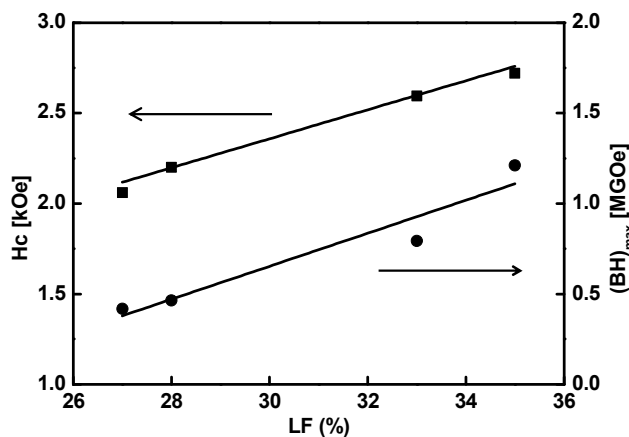


**Fig. 8** Relationship of magnetic NP alignment with magnetic properties of  $\alpha''$ -Fe<sub>16</sub>N<sub>2</sub> NP film.

The magnetic properties of the horizontally aligned film (sample H) are shown by the demagnetization field corrected hysteresis loop in Fig. 7b. The application of a magnetic field of 0.6 T in the horizontal direction impairs the magnetic properties [ $M_r/M_s$ ,  $H_c$ , and  $(BH)_{max}$  values of 0.32, 2.1 kOe, and 0.42 MG Oe, respectively] compared with those of the film sample prepared without a magnetic field (sample V0). These results show that the magnetic properties of the  $\alpha''$ -Fe<sub>16</sub>N<sub>2</sub> magnetic film are governed by the alignment of the magnetic orientation of the NPs, which can be controlled by applying an external magnetic field during film preparation. The relationship between the alignment of the magnetic orientation of the  $\alpha''$ -Fe<sub>16</sub>N<sub>2</sub> NPs and the magnetic performance of the film, as shown in Fig. 8, confirms that both  $H_c$  and  $(BH)_{max}$  increased with increasing the alignment of the magnetic orientation. It was estimated that the maximum  $H_c$  and  $(BH)_{max}$  values were approximately 8 kOe and 7 MG Oe, respectively, at the perfect alignment. The low value of  $(BH)_{max}$  value may arise from the presence of resin in the film. These results are important for the development of spintronic device applications and also suggest the possibility of the nanostructuring of bulk anisotropic magnetic materials by magnetic field induced compaction of single-domain  $\alpha''$ -Fe<sub>16</sub>N<sub>2</sub> NPs.

## Conclusions

The magnetic field induced single domain core-shell  $\alpha''$ -Fe<sub>16</sub>N<sub>2</sub> NP films show densely packed NP assemblies. The XRD and SQUID analysis show increases in the alignment of the magnetic orientation of the NPs and the magnetic properties with the increase in the magnetic field applied vertically to the film substrate. At 1.2 T, the alignment of the magnetic orientation increased by 35%, whereas the  $H_c$ ,  $M_r$ , and  $(BH)_{max}$  increased by 24%, 66%, and 160%, respectively. The maximum

$H_c$  and  $(BH)_{max}$  values can be estimated from the relationship between the alignment of the magnetic orientation and the magnetic properties to be approximately 8 kOe and 7 MG Oe, respectively. These results imply that core-shell  $\alpha''$ -Fe<sub>16</sub>N<sub>2</sub>/Al<sub>2</sub>O<sub>3</sub> NPs have the potential for the construction of bulk magnetic materials with controllable magnetic performances by applying a magnetic field.

## Acknowledgements

This work was partly supported by the Research and Development of Alternative New Permanent Magnetic Materials to Nd-Fe-B Magnets Project from NEDO of Japan, the Japanese National Project of Technology Research Association of Magnetic Materials for High-Efficiency Motors for Next-Generation Cars. The authors also gratefully acknowledge the Ministry of Education, Culture, Sports, Science, and Technology (MEXT) of Japan for providing scholarships (C.W.K. and R.Z.). The authors further thank Professor Dr. Toshiro Takabatake and Associate Professor Dr. Takahiro Onimaru from the Department of Quantum Matter, Graduate School of Advanced Sciences of Matter, Hiroshima University, for the SQUID measurements.

## References

1. S. Sun, *Adv. Mater.*, 2006, **18**, 393-403.
2. R. Zulhijah, K. Yoshimi, A. B. D. Nandiyanto, T. Ogi, T. Iwaki, K. Nakamura and K. Okuyama, *Adv. Powder Technol.*, 2014, **25**, 582-590.
3. O. Akdogan, W. Li, B. Balasubramanian, D. J. Sellmyer and G. C. Hadjipanayis, *Adv. Funct. Mater.*, 2013, **23**, 3262-3267.
4. N. Poudyal and J. Ping Liu, *J. Phys. D Appl. Phys.*, 2013, **46**, 043001.
5. C. Chappert, A. Fert and F. N. Van Dau, *Nat. Mater.*, 2007, **6**, 813-823.
6. D. J. Sellmyer, *Nature*, 2002, **420**, 374-375.
7. B. Balamurugan, B. Das, P. Mukherjee and D. Sellmyer, *Sripta Mater.*, 2014, **67**, 542-547.
8. B. Issa, I. M. Obaidat, B. A. Albiss and Y. Haik, *Int. J. Mol. Sci.*, 2013, **14**, 21266-21305.
9. N. A. Frey, S. Peng, K. Cheng and S. Sun, *Chem. Soc. Rev.*, 2009, **38**, 2532-2542.
10. B. Balamurugan, D. J. Sellmyer, G. C. Hadjipanayis and R. Skomski, *Sripta Mater.*, 2012, **67**, 542-547.
11. C. T. Black, C. B. Murray, R. L. Sandstrom and S. Sun, *Science*, 2000, **290**, 1131-1134.
12. S. Singamaneni, V. N. Bliznyuk, C. Binek and E. Y. Tsymlal, *J. Mater. Chem.*, 2011, **21**, 16819.
13. T. Fried, G. Shemer and G. Markovich, *Adv. Mater.*, 2001, **13**, 1158-1161.
14. T. Ogi, A. B. Dani Nandiyanto, Y. Kisakibaru, T. Iwaki, K. Nakamura and K. Okuyama, *J. Appl. Phys.*, 2013, **113**, 164301.
15. R. Zulhijah, A. B. Dani Nandiyanto, T. Ogi, T. Iwaki, K. Nakamura and K. Okuyama, *Nanoscale*, 2014, **6**, 6487-6891.

16. R. Zulhijah, A. B. D. Nandiyanto, T. Ogi, T. Iwaki, K. Nakamura and K. Okuyama, *J. Magn. Magn. Mater.*, 2015, **381**, 89-98.
17. S. Bhattacharyya, *J. Phys. Chem. C*, 2015, **119**, 1601-1622.
18. J. Dugay, R. P. Tan, A. Loubat, L. M. Lacroix, J. Carrey, P. F. Fazzini, T. Blon, A. Mayoral, B. Chaudret and M. Respaud, *Langmuir*, 2014, **30**, 9028-9035.
19. R. Zulhijah, A. Suhendi, K. Yoshimi, C. W. Kartikowati, T. Ogi, T. Iwaki and K. Okuyama, *Langmuir*, 2015, **31**, 6011-6019.
20. A. Suhendi, C. W. Kartikowati, R. Zulhijah, T. Ogi, T. Iwaki and K. Okuyama, DOI: 10.1016/j.appt.2015.09.005.
21. R. Furushima, S. Tanaka, Z. Kato and K. Uematsu, *J. Ceram. Soc. Jpn.*, 2010, **118**, 921-926.
22. J. Wang, Q. Chen, C. Zeng and B. Hou, *Adv. Mater.*, 2004, **16**, 137-140.
23. J. Wang, Q. Chen, X. Li, L. Shi, Z. Peng and C. Zeng, *Chem. Phys. Lett*, 2004, **390**, 55-58.
24. Y. Su, Y. Zhang, H. Wei, L. Zhang, J. Zhao, Z. Yang and Y. Zhang, *Nanoscale*, 2012, **4**, 1717-1721.
25. M. Keidar, I. Levchenko, T. Arbel, M. Alexander, A. M. Waas and K. Ostrikov, *Appl. Phys. Lett*, 2008, **92**, 043129.
26. Y. Su, Y. Zhang, H. Wei, Z. Yang, E. S.-W. Kong and Y. Zhang, *Carbon*, 2012, **50**, 2556-2562.
27. S. Morup, M. F. Hansen and C. Frandsen, *Beilstein J. Nanotechnol.*, 2010, **1**, 182-190.
28. T. K. Kim and M. Takahashi, *Appl. Phys. Lett*, 1972, **20**, 492.
29. Y. Sugita, H. Takahashi, M. Komuro, M. Igarashi, R. Imura and T. Kambe, *J. Appl. Phys.*, 1996, **79**, 5576.
30. M. Takahashi, H. Shoji, H. Takahashi, T. Wakiyama, M. Kinoshita and W. Ohta, *Magnetics, IEEE Transactions on*, 1993, **29**, 3040-3045.
31. D. Kechrakos and K. N. Trohidou, *J. Magn. Magn. Mater.*, 2003, **262**, 107-110.
32. H. R. Kirchmayr, *J. Phys. D Appl. Phys.*, 1996, **29**, 2763-2778.
33. L. Hu, R. Zhang and Q. Chen, *Nanoscale*, 2014, **6**, 14064-14105.